

Bayesian CRLB for hybrid ToA and DoA based wireless localization with anchor uncertainty

Samuel Van de Velde*, Giuseppe Abreu†, and Heidi Steendam*

*TELIN department, Ghent University, Belgium, e-mail: {slvdveld, hs}@telin.ugent.be

†School of Engineering and Science, Jacobs University Bremen, Germany, e-mail: g.abreu@jacobs-university.de

Abstract—In this paper, we derive the Bayesian Cramér-Rao lower bound for three dimensional hybrid localization using time-of-arrival (ToA) and direction-of-arrival (DoA) types of measurements. Unlike previous works, we include the practical constraint that the anchor position is not known exactly but rather up to some error. The resulting bound can be used for error analysis of such a localization system or as an optimality criterion for the selection of suitable anchors.

Index Terms—Bayesian CRLB, anchor uncertainty, hybrid, localization

I. INTRODUCTION

Accurately knowing the positions of wireless network nodes is essential for many current and next-generation applications in automotive, military and public service systems. GPS technology has been very successful in providing rough positioning information suitable for outdoor navigation. However, due to reduced satellite reception, the GPS system cannot provide reliable positioning information indoors. Because of this, terrestrial localization solutions have gained success in situations where GPS falls short. In wireless localization, a target position can be obtained by measuring position related signals with respect to a number of nodes in the network. Common types of measurements are the distance, angle or signal strength. In order to obtain absolute positioning information, the position of the network nodes must be known and the nodes are referred to as anchors (or reference points). For example, in GPS, the satellites which follow an accurately determined trajectory around the earth act as (moving) anchors.

Apart from the actual position estimation, a large amount of research has focused its attention on formulating fundamental limits on the achievable positioning accuracy. These limits can serve as a benchmark for localization or as a criterion for anchor selection [1], [2]. Furthermore, because the localization accuracy strongly depends on the geometry of the network, the bounds can be used to solve the optimal anchor placement problem [3][4]. A widely used fundamental bound is the Cramér-Rao lower bound (CRLB) which bounds the achievable variance of an unbiased estimate [5]. In [6], the CRLB for time-of-arrival (ToA), i.e., distance-based, localization is presented for multiple cooperating targets. In [7], the bound is applied to ultra-wideband signals and in [4], the CRLB for direction-of-arrival (DoA) is derived. In all of the above works, the position of the anchors is considered to be known exactly. However, in practical scenarios, this is rarely the case. For example, the position of the anchor can be measured by

means of GPS, or using the simultaneous localization and mapping (SLAM) principle, where a mobile robot estimates the position of the anchors by driving around in the area. Even in the common case where the anchor position is measured manually, it remains subject to some error. In [8], the CRLB for ToA-based wireless localization is derived for anchors with a Gaussian position uncertainty.

In this work, we generalize this for hybrid ToA and DoA based localization where the anchor uncertainty can have an arbitrary distribution. It turns out that the derivation of this bound is conceptually different from [8]. The generalization for arbitrary distributions is not only valuable from a theoretic point of view, it also has a practical application in that it can be used when the anchor position is described by particles (for example, as a result of a particle based estimation of the anchor).

II. PROBLEM STATEMENT

A. System model

Consider a wireless network in which the target user has coordinates $\mathbf{x}_t \in \mathbb{R}^\eta$ with $\eta = 2, 3$ for two or three dimensional localization, respectively. The target user is wirelessly connected to $M + N$ neighboring anchors with coordinates $\mathbf{x}_k^{\text{ref}} \in \mathbb{R}^\eta$ where $k = 1, 2, \dots, M + N$. Let us consider that the first M anchors have uncertain position information and the last N anchors have exact position information. We assume that for the inaccurate anchors, the distribution $p_k(\mathbf{x}_k^{\text{ref}})$ of the position is known for the respective k th anchor. An example network is shown in Fig. 1 for $M = 5$ and $N = 1$.

The target user can make both distance (ToA) measurements r_k and bearing (DoA) measurements \mathbf{b}_k with the k th anchor, modeled by

$$r_k = \|\mathbf{x}_t - \mathbf{x}_k^{\text{ref}}\| + \zeta_k \quad (1)$$

$$\mathbf{b}_k = \frac{\mathbf{x}_t - \mathbf{x}_k^{\text{ref}}}{\|\mathbf{x}_t - \mathbf{x}_k^{\text{ref}}\|} + \boldsymbol{\xi}_k \quad (2)$$

with ζ_k and $\boldsymbol{\xi}_k$ terms that represent possible errors resulting from measurement noise, hardware imperfections and signal modeling inaccuracies. We model ζ_k and $\boldsymbol{\xi}_k$ as zero mean normally distributed noise with variance σ_r^2 and $\sigma_b^2 \mathbf{I}_\eta$, respectively. The collection of all measurements is denoted by \mathbf{z} . Furthermore, the prior distribution of the target is given by $p_0(\mathbf{x}_t)$.

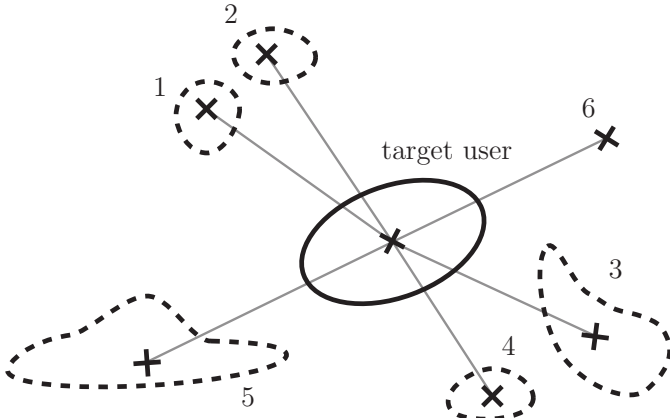


Figure 1. System setup with $M = 5$ inaccurate anchors and $N = 1$ precise anchor. The dashed boundaries represent the 95% confidence regions for the uncertain anchors' positions. The solid ellipse represents the 95% confidence region of the prior distribution of the target.

III. BAYESIAN CRLB

A. Preliminaries

Before we consider the anchor uncertainty, let us formulate the Bayesian CRLB for hybrid DoA and ToA localization. In the next subsection, we will build upon this bound to derive the CRLB with anchor uncertainty.

Using the system model from the previous section, we can describe the posterior distribution $p(\mathbf{x}_t|\mathbf{z})$ of \mathbf{x}_t given the measurements \mathbf{z} . Without anchor uncertainty, i.e., for $M = 0$, we obtain the following posterior distribution of the target position:

$$p(\mathbf{x}_t|\mathbf{z}) \propto p(\mathbf{z}|\mathbf{x}_t)p_0(\mathbf{x}_t) \quad (3)$$

$$= \prod_{k=1}^N p_k(\mathbf{z}_k|\mathbf{x}_t)p_0(\mathbf{x}_t) \quad (4)$$

$$= \prod_{k=1}^N p_k(r_k|\mathbf{x}_t)p_k(\mathbf{b}_k|\mathbf{x}_t)p_0(\mathbf{x}_t) \quad (5)$$

with $p_k(r_k|\mathbf{x}_t) = \mathcal{N}(r_k; \|\mathbf{x}_t - \mathbf{x}_k^{\text{ref}}\|, \sigma_r^2)$ and $p_k(\mathbf{b}_k|\mathbf{x}_t) = \mathcal{N}(\mathbf{b}_k; \frac{\mathbf{x}_t - \mathbf{x}_k^{\text{ref}}}{\|\mathbf{x}_t - \mathbf{x}_k^{\text{ref}}\|}, \Sigma_b)$.

It is well-known [5] that the covariance matrix of an unbiased estimate $\hat{\mathbf{x}}_t(\mathbf{z})$ is bounded by the BCRLB as follows

$$\mathbf{C}_{\hat{\mathbf{x}}_t} = \mathbb{E}_{\mathbf{z}, \mathbf{x}_t} \left[(\mathbf{x}_t - \hat{\mathbf{x}}_t(\mathbf{z})) (\mathbf{x}_t - \hat{\mathbf{x}}_t(\mathbf{z}))^T \right] \succeq \mathbf{F}_t^{-1} \quad (6)$$

where $\mathbb{E}_{\mathbf{z}, \mathbf{x}_t}[\cdot]$ denotes the expectation over the distribution of \mathbf{z} and \mathbf{x}_t , the symbol \succeq denotes positive-semidefinite inequality and \mathbf{F}_t^{-1} is the inverse of the Bayesian Fisher information matrix (BFIM) of \mathbf{x}_t . In turn, the BFIM of \mathbf{x}_t , using the posterior distribution in (3), is given by

$$\begin{aligned} \mathbf{F}_t &\triangleq -\mathbb{E}_{\mathbf{z}, \mathbf{x}_t} \left[\frac{\partial^2 \log p(\mathbf{x}_t|\mathbf{z})}{\partial \mathbf{x}_t^2} \right] \\ &= -\mathbb{E}_{\mathbf{x}_t} \left[\frac{\partial^2 \log p_0(\mathbf{x}_t)}{\partial \mathbf{x}_t^2} \right] - \mathbb{E}_{\mathbf{z}, \mathbf{x}_t} \left[\sum_{k=1}^{M+N} \frac{\partial^2 \log p(\mathbf{z}_k|\mathbf{x}_t)}{\partial \mathbf{x}_t^2} \right] \\ &= \mathbf{\Omega}_t + \mathbb{E}_{\mathbf{x}_t} \left[\sum_{k=1}^{M+N} \mathbf{H}(\mathbf{x}_t, \mathbf{x}_k^{\text{ref}}) \right] \end{aligned} \quad (7)$$

where $\mathbf{\Omega}_t = -\mathbb{E}_{\mathbf{x}_t} \left[\frac{\partial^2 \log p_0(\mathbf{x}_t)}{\partial \mathbf{x}_t^2} \right]$, which will be large whenever the prior distribution is concentrated. The $\eta \times \eta$ matrix $\mathbf{H}(\mathbf{x}_t, \mathbf{x}_k^{\text{ref}}) = \mathbb{E}_{\mathbf{z}} \left[\frac{\partial^2 \log p(\mathbf{z}_k|\mathbf{x}_t)}{\partial \mathbf{x}_t^2} \right]$ can be obtained for distance and bearings measurements in [3] and [4], respectively. Using the shorthand notation $\mathbf{p}_k = \mathbf{x}_t - \mathbf{x}_k^{\text{ref}}$, we obtain $\mathbf{H}(\mathbf{x}_t, \mathbf{x}_k^{\text{ref}}) = \mathbf{H}_r(\mathbf{p}_k) + \mathbf{H}_b(\mathbf{p}_k)$ where

$$\mathbf{H}_r(\mathbf{p}_k) \triangleq \mathbb{E}_{r_k} \left[\frac{\partial^2 \log p_k(r_k|\mathbf{x}_t)}{\partial \mathbf{x}_t^2} \right] = \frac{1}{\sigma_r^2} \frac{\mathbf{p}_k \mathbf{p}_k^T}{\|\mathbf{p}_k\|^2} \quad (8)$$

$$\mathbf{H}_b(\mathbf{p}_k) \triangleq \mathbb{E}_{\mathbf{b}_k} \left[\frac{\partial^2 \log p_k(\mathbf{b}_k|\mathbf{x}_t)}{\partial \mathbf{x}_t^2} \right] = \frac{(\mathbf{I}_\eta - \frac{\mathbf{p}_k \mathbf{p}_k^T}{\|\mathbf{p}_k\|^2})}{\sigma_b^2 \|\mathbf{p}_k\|^2} \quad (9)$$

with \mathbf{I}_η the $\eta \times \eta$ identity matrix. The positive definite \mathbf{H} -matrices can be seen as the basic building blocks of the FIM for localization. Each $\mathbf{H}(\mathbf{x}_t, \mathbf{x}_k^{\text{ref}})$ describes the amount of information resulting from the measurements made with the k th anchor.

B. Anchor uncertainty

With uncertainty over the position of the anchors, the estimation is no longer governed by the posterior distribution in (3). To introduce the uncertainties of the anchors, we consider the joint posterior distribution of the target and uncertain anchors. Define $\boldsymbol{\theta} = [\mathbf{x}_t, \mathbf{x}_{1:M}^{\text{ref}}]$, where $\mathbf{x}_{1:M}^{\text{ref}}$ represents the anchor positions $\mathbf{x}_k^{\text{ref}}$ for $k = 1..M$. We can factorize the joint posterior distribution of $\boldsymbol{\theta}$ given the measurements \mathbf{z} using Bayes' rule:

$$\begin{aligned} p(\boldsymbol{\theta}|\mathbf{z}) &\propto p(\mathbf{z}|\boldsymbol{\theta})p(\boldsymbol{\theta}) \\ &= p(\mathbf{z}|\boldsymbol{\theta})p_0(\mathbf{x}_t) \prod_{k=1}^M p_k(\mathbf{x}_k^{\text{ref}}) \end{aligned} \quad (10)$$

Now, the marginal distribution of the target position can be obtained by marginalizing out all the uncertain anchors $\mathbf{x}_{1:M}^{\text{ref}}$

$$p(\mathbf{x}_t|\mathbf{z}) \propto \int p(\boldsymbol{\theta}|\mathbf{z}) d\mathbf{x}_{1:M}^{\text{ref}}. \quad (11)$$

A method to obtain a bound for the estimation that uses the marginal distribution of \mathbf{x}_t can be obtained by considering the Bayesian CRLB for the target and the M imprecise anchors jointly. Similar to (6), the Bayesian CRLB bound on the covariance matrix of an unbiased estimate $\hat{\boldsymbol{\theta}}(\mathbf{z})$ is given by

$$\mathbf{C}_{\hat{\boldsymbol{\theta}}} = \mathbb{E}_{\mathbf{z}, \boldsymbol{\theta}} \left[(\boldsymbol{\theta} - \hat{\boldsymbol{\theta}}(\mathbf{z})) (\boldsymbol{\theta} - \hat{\boldsymbol{\theta}}(\mathbf{z}))^T \right] \succeq \mathbf{F}_{\boldsymbol{\theta}}^{-1} \quad (12)$$

with \mathbf{F}_θ^{-1} is the inverse of the Bayesian Fisher information matrix of θ . Equation (12) states that $\mathbf{C}_\theta - \mathbf{F}_\theta^{-1}$ must be a positive-semidefinite matrix. As per definition this means that $\mathbf{y}^T(\mathbf{C}_\theta - \mathbf{F}_\theta^{-1})\mathbf{y} \geq 0$ for any $\mathbf{y} \in \mathbb{R}^{\eta(M+1)}$. If we set $\mathbf{y} = [\mathbf{v}^T, \mathbf{0}]^T$ with $\mathbf{v} \in \mathbb{R}^\eta$ and we define $\mathbf{C}_{\hat{\mathbf{x}}_t}$ and $\tilde{\mathbf{F}}_t^{-1}$ as the $\eta \times \eta$ upper-left blocks of \mathbf{C}_θ and \mathbf{F}_θ^{-1} , respectively, we can write $\mathbf{y}^T(\mathbf{C}_\theta - \mathbf{F}_\theta^{-1})\mathbf{y} = \mathbf{v}^T(\mathbf{C}_{\hat{\mathbf{x}}_t} - \tilde{\mathbf{F}}_t^{-1})\mathbf{v} \geq 0$. Hence, $\mathbf{C}_{\hat{\mathbf{x}}_t} - \tilde{\mathbf{F}}_t^{-1}$ is positive-semidefinite and we obtain a bound on the covariance of any unbiased estimate $\hat{\mathbf{x}}_t(\mathbf{z})$:

$$\mathbf{C}_{\hat{\mathbf{x}}_t} = \mathbb{E}_{\mathbf{z}, \theta} \left[(\mathbf{x}_t - \hat{\mathbf{x}}_t(\mathbf{z})) (\mathbf{x}_t - \hat{\mathbf{x}}_t(\mathbf{z}))^T \right] \succeq \tilde{\mathbf{F}}_t^{-1}. \quad (13)$$

It must be stressed that the matrix $\tilde{\mathbf{F}}_t$ is –in general– not the same as the Bayesian FIM \mathbf{F}_t in (7). In order to make this distinction more clear we will call the matrix $\tilde{\mathbf{F}}_t$ the *marginal* FIM of \mathbf{x}_t . In order to derive an expression for the marginal FIM $\tilde{\mathbf{F}}_t$, we first derive the $\eta(M+1) \times \eta(M+1)$ Bayesian Fisher information matrix (FIM) of θ , defined as [9]:

$$\begin{aligned} \mathbf{F}_\theta &\triangleq -\mathbb{E}_{\mathbf{z}, \theta} \left[\frac{\partial^2 \log p(\theta | \mathbf{z})}{\partial \theta^2} \right] \\ &= -\mathbb{E}_{\mathbf{z}, \theta} \left[\frac{\partial^2 \log p(\mathbf{z} | \theta)}{\partial \theta^2} \right] - \mathbb{E}_\theta \left[\frac{\partial^2 \log p(\theta)}{\partial \theta^2} \right] \\ &= \mathbb{E}_\theta [\mathbf{F}_{\text{nb}, \theta}] + \mathbf{F}_p \end{aligned} \quad (14)$$

with $\mathbf{F}_{\text{nb}, \theta}$ the non-Bayesian FIM of θ and \mathbf{F}_p a term related to the prior information of θ . Because the distributions of the anchor positions are independent, the matrix \mathbf{F}_p is a block-diagonal matrix with each $\eta \times \eta$ block equal to the Fisher information of the corresponding node, i.e., $\mathbf{F}_p = \text{diag}(\Omega_t, \Omega_a)$ with $\Omega_a = \text{diag}(\Omega_1, \Omega_2, \dots, \Omega_M)$ and $\Omega_k = -\mathbb{E}_{\mathbf{x}_k} \left[\frac{\partial^2 \log p_k(\mathbf{x}_k^{\text{ref}})}{\partial (\mathbf{x}_k^{\text{ref}})^2} \right]$ for $k = 1..M$. The non-Bayesian FIM $\mathbf{F}_{\text{nb}, \theta}$ is compactly given as [3]:

$$\mathbf{F}_{\text{nb}, \theta} = \begin{bmatrix} \mathbf{A} & -\mathbf{B}^T \\ -\mathbf{B} & \mathbf{C} \end{bmatrix} \quad (15)$$

with

$$\mathbf{A} = \sum_{k=1}^{M+N} \mathbf{H}(\mathbf{x}_t, \mathbf{x}_k) \quad (16)$$

$$\mathbf{B} = [\mathbf{H}(\mathbf{x}_t, \mathbf{x}_1), \dots, \mathbf{H}(\mathbf{x}_t, \mathbf{x}_M)]^T \quad (17)$$

$$\mathbf{C} = \text{diag}(\mathbf{H}(\mathbf{x}_t, \mathbf{x}_1), \dots, \mathbf{H}(\mathbf{x}_t, \mathbf{x}_M)) \quad (18)$$

The formulation of the non-Bayesian FIM $\mathbf{F}_{\text{nb}, \theta}$ of the joint parameters can easily be understood by considering the building blocks $\mathbf{H}(\mathbf{x}_t, \mathbf{x}_k)$. More specifically, the diagonal $\eta \times \eta$ blocks in (15) correspond to measurements made as if all neighbors have perfect positioning information. In other words, the diagonal blocks resemble the information without uncertainty of the nodes positions and is overly optimistic. The off-diagonal blocks in (15) represent the interactions between the nodes, and make a correction for this. Because the anchors do not interact, i.e. they do not exchange measurements, the matrix \mathbf{C} is simply a block-diagonal matrix. By inserting (15) into (14), the Bayesian FIM \mathbf{F}_θ can be written as

$$\begin{aligned} \mathbf{F}_\theta &= \begin{bmatrix} \mathbb{E}_\theta[\mathbf{A}] + \Omega_t & -\mathbb{E}_\theta[\mathbf{B}^T] \\ -\mathbb{E}_\theta[\mathbf{B}] & \mathbb{E}_\theta[\mathbf{C}] + \Omega_a \end{bmatrix} \\ &\triangleq \begin{bmatrix} \tilde{\mathbf{A}} + \Omega_t & -\tilde{\mathbf{B}}^T \\ -\tilde{\mathbf{B}} & \tilde{\mathbf{C}} + \Omega_a \end{bmatrix}. \end{aligned} \quad (19)$$

The desired \mathbf{F}_t^{-1} is now obtained by taking the $\eta \times \eta$ upper-left block of \mathbf{F}_θ^{-1} . Rather than inverting the whole matrix \mathbf{F}_θ , however, we can take the Schur complement of the lower-right block of \mathbf{F}_θ in (19), which exactly corresponds to the inverse of $\tilde{\mathbf{F}}_t^{-1}$ (or simply $\tilde{\mathbf{F}}_t$). More specifically:

$$\tilde{\mathbf{F}}_t = (\tilde{\mathbf{A}} + \Omega_t) - \tilde{\mathbf{B}}^T (\tilde{\mathbf{C}} + \Omega_a)^{-1} \tilde{\mathbf{B}} \quad (20)$$

Due to the linearity of the expectation operator, we obtain $\tilde{\mathbf{A}} = \sum_{k=1}^{M+N} \Psi_k$, $\tilde{\mathbf{B}} = [\Psi_1, \dots, \Psi_M]^T$ and $\tilde{\mathbf{C}} = \text{diag}(\Psi_1, \dots, \Psi_M)$, where $\Psi_k = \mathbb{E}_{\mathbf{x}_t, \mathbf{x}_k} [\mathbf{H}(\mathbf{x}_t, \mathbf{x}_k)]$. Inserting this into (20) results in

$$\begin{aligned} \tilde{\mathbf{F}}_t &= \Omega_t + \sum_{k=1}^{M+N} \Psi_k - \tilde{\mathbf{B}}^T (\tilde{\mathbf{C}} + \Omega_n)^{-1} \tilde{\mathbf{B}} \\ &= \Omega_t + \sum_{k=M+1}^{M+N} \Psi_k + \sum_{k=1}^M (\Psi_k - \Psi_k (\Psi_k + \Omega_k)^{-1} \Psi_k) \\ &= \underbrace{\Omega_t}_{\text{prior}} + \underbrace{\sum_{k=M+1}^{M+N} \Psi_k}_{\text{precise anchors}} + \underbrace{\sum_{k=1}^M (\Psi_k^{-1} + \Omega_k^{-1})^{-1}}_{\text{imprecise anchors}}. \end{aligned} \quad (21)$$

In the last equation, we used the Woodbury identity¹, which is allowed only if Ψ_k and Ω_k have an inverse. This is true because the expected value results in an infinite sum of different rank one matrices, resulting in full rank and thus invertible matrices Ψ_k and Ω_k , for $k \leq M$.

In case the prior distribution of the target and the distributions of the imprecise anchors are Gaussian, i.e., $p_0(\mathbf{x}_t) = \mathcal{N}(\boldsymbol{\mu}_t, \boldsymbol{\Sigma}_t)$ and $p_k(\mathbf{x}_k) = \mathcal{N}(\boldsymbol{\mu}_k, \boldsymbol{\Sigma}_k)$, we obtain a closed form expression for the terms Ω_t and Ω_k , i.e., $\Omega_t = \boldsymbol{\Sigma}_t^{-1}$ and $\Omega_k = \boldsymbol{\Sigma}_k^{-1}$. This results in the marginal FIM for the Gaussian approximation:

$$\tilde{\mathbf{F}}_t = \boldsymbol{\Sigma}_t^{-1} + \sum_{k=M+1}^{M+N} \Psi_k + \sum_{k=1}^M (\Psi_k^{-1} + \boldsymbol{\Sigma}_k)^{-1}. \quad (22)$$

C. Effect of uncertainty

In order to understand the effect that the uncertainty of the anchors has on the performance of localization, we consider the bound in case the the measurement noise goes to zero. For this we evaluate the trace of the inequality in (13) which results in a bound on the mean squared error (MSE), i.e., $\text{MSE}(\hat{\mathbf{x}}_t) > \text{tr} \tilde{\mathbf{F}}_t^{-1}$.

Let us consider ToA-based localization only, although the same derivation is valid for DoA-based localization. By using

¹The Woodbury identity is given by: $(\mathbf{A} + \mathbf{UBV})^{-1} = \mathbf{A}^{-1} - \mathbf{A}^{-1} \mathbf{U} (\mathbf{B}^{-1} + \mathbf{VA}^{-1} \mathbf{U})^{-1} \mathbf{VA}^{-1}$.

equation (8) and the definition of Ψ_k for ToA-based localization, we can write:

$$\Psi_k = \frac{1}{\sigma_r^2} \mathbb{E}_{\mathbf{x}_t, \mathbf{x}_k^{\text{ref}}} \left[\frac{\mathbf{p}_k \mathbf{p}_k^T}{\|\mathbf{p}_k\|^2} \right]. \quad (23)$$

First we consider the bound on the MSE when there is no uncertainty in the anchor positions, i.e., $M = 0$, and we let the measurement noise go to zero.

$$\begin{aligned} \lim_{\sigma_r^2 \rightarrow 0} \text{tr} \tilde{\mathbf{F}}_{M=0}^{-1} &= \lim_{\sigma_r^2 \rightarrow 0} \text{tr} \left(\Omega_t + \sum_{k=1}^N \Psi_k \right)^{-1} \\ &= \lim_{\sigma_r^2 \rightarrow 0} \text{tr} \left(\Omega_t + \frac{1}{\sigma_r^2} \mathbf{K} \right)^{-1} \\ &= \lim_{\sigma_r^2 \rightarrow 0} \text{tr} \left(\sigma_r^2 \mathbf{K}^{-1} - \sigma_r^4 \mathbf{K}^{-1} (\sigma_r^2 \mathbf{K}^{-1} + \Omega_t^{-1})^{-1} \mathbf{K}^{-1} \right) \\ &= 0 \end{aligned} \quad (24)$$

where $\mathbf{K} = \sum_{k=1}^M \frac{\mathbf{p}_k \mathbf{p}_k^T}{\|\mathbf{p}_k\|^2}$. As we expected, we see from (24) that, if \mathbf{K}^{-1} exists, the bound on the MSE goes to zero when there is no noise in the measurements. Whenever \mathbf{K} is singular, which is true when all anchors are collinear on a line that goes through the target, the limit does not go to zero but rather to infinity, corresponding to an ill-chosen geometry of the anchors.

Similarly for the case where all anchors have uncertainty, i.e., $N = 0$, we write the bound on the MSE when the measurement noise goes to zero:

$$\begin{aligned} \lim_{\sigma_r^2 \rightarrow 0} \text{tr} \tilde{\mathbf{F}}_{N=0}^{-1} &= \lim_{\sigma_r^2 \rightarrow 0} \text{tr} \left(\Omega_t + \sum_{k=1}^M (\Psi_k^{-1} + \Omega_k^{-1})^{-1} \right)^{-1} \\ &= \text{tr} \left(\Omega_t + \sum_{k=1}^M \Omega_k \right)^{-1} \end{aligned} \quad (25)$$

With anchor uncertainty, we see that the bound on the MSE does not go zero. In fact, the uncertainty in the anchors' positions is transferred to the uncertainty in the target position. For the Gaussian case where $\Omega_t = \frac{1}{\sigma_t^2} \mathbf{I}_\eta$ and all anchors have equal uncertainty $\Omega_k = \frac{1}{\sigma_p^2} \mathbf{I}_\eta$, we can write equation (25) as follows:

$$\begin{aligned} \lim_{\sigma_r^2 \rightarrow 0} \text{tr} \tilde{\mathbf{F}}_{N=0}^{-1} &= \text{tr} \left(\frac{1}{\sigma_t^2} \mathbf{I}_\eta + \sum_{k=1}^M \frac{1}{\sigma_p^2} \mathbf{I}_\eta \right)^{-1} \\ &= \frac{\sigma_t^2 \sigma_p^2}{M \sigma_t^2 + \sigma_p^2} \eta \end{aligned} \quad (26)$$

Here we see that if we increase the number of anchors, the bound of the MSE will decrease.

IV. NUMERICAL RESULTS

A. Simulation setup

In simulation setup, the target user is surrounded with $M = 6$ imprecise anchors. The prior of the target is $\mathcal{N}(\mathbf{0}, \sigma_t^2 \mathbf{I}_2)$ with $\sigma_t = 0.5\text{m}$ and the prior of the anchors is $\mathcal{N}(\boldsymbol{\mu}_m, \sigma_n^2 \mathbf{I}_2)$ with

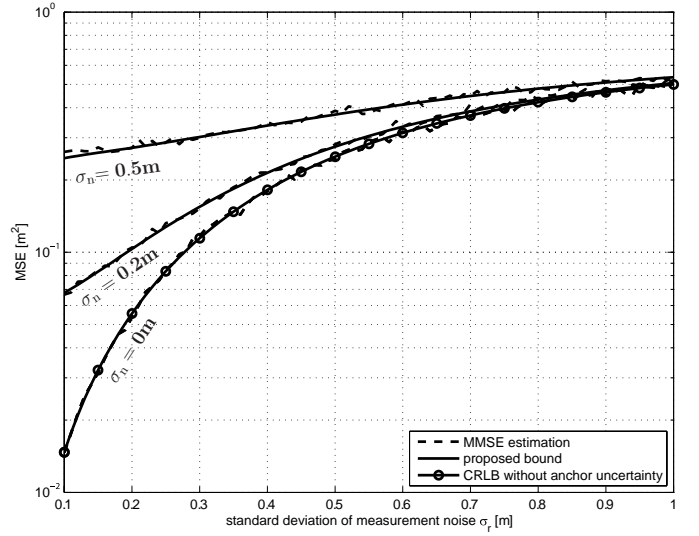


Figure 2. Evaluation of the bound for distance-based localization for an uncertainty on the neighbors' positions varying between $\sigma_n = \{0\text{m}, 0.2\text{m}, 0.5\text{m}\}$.

$\boldsymbol{\mu}_1 = [R, 0, 0]^T$, $\boldsymbol{\mu}_2 = [-R, 0, 0]^T$, $\boldsymbol{\mu}_3 = [0, R, 0]^T$, $\boldsymbol{\mu}_4 = [0, -R, 0]^T$, $\boldsymbol{\mu}_5 = [0, 0, R]^T$ and $\boldsymbol{\mu}_6 = [0, 0, -R]^T$. In order to evaluate the bound, we compute the minimum mean squared error (MMSE) position estimate $\hat{\mathbf{x}}_{\text{MMSE}} = \mathbb{E}_{p(\mathbf{x}_t|\mathbf{z})} [\mathbf{x}_t]$ by means of importance sampling. Using equations (11) and (10), we can write the MMSE estimate as follows:

$$\begin{aligned} \hat{\mathbf{x}}_{\text{MMSE}} &\triangleq \int \mathbf{x}_t p(\mathbf{x}_t|\mathbf{z}) d\mathbf{x}_t = \int \mathbf{x}_t p(\boldsymbol{\theta}|\mathbf{z}) d\boldsymbol{\theta} \quad (27) \\ &= \int \mathbf{x}_t p(\mathbf{z}|\boldsymbol{\theta}) p_0(\mathbf{x}_t) \underbrace{\prod_{k=1}^M p_k(\mathbf{x}_k^{\text{ref}})}_{\text{proposal } q(\boldsymbol{\theta})} d\boldsymbol{\theta} \quad (28) \end{aligned}$$

The integral in (28) can be approximated by means of importance sampling. For the approximation, we use $q(\boldsymbol{\theta}) = p_0(\mathbf{x}_t) \prod_{k=1}^M p_k(\mathbf{x}_k^{\text{ref}})$ as the proposal distribution. This results in

$$\hat{\mathbf{x}}_{\text{MMSE}} \approx \frac{1}{L} \sum_{\ell=1}^L \mathbf{x}^\ell w^\ell \quad (29)$$

with $\boldsymbol{\theta}^\ell \sim q(\boldsymbol{\theta})$ and the weights $w^\ell = \mathbf{x}_t^\ell p(\mathbf{z}|\boldsymbol{\theta}^\ell)$ for $\ell = 1..L$, and L the number of samples. The number of samples must be chosen sufficiently high for a good approximation. In general, more samples will be required when the proposal distribution is broad and the measurements are made with low noise. For this simulation setup, $L = 10000$ is selected to cover all parameters².

B. Results

The BCRLB, computed with (22), is compared with the mean squared error (MSE) of the MMSE estimates obtained

²The simulations are designed to test the bound, because of this, a very large number of samples is chosen to minimize the estimation error.

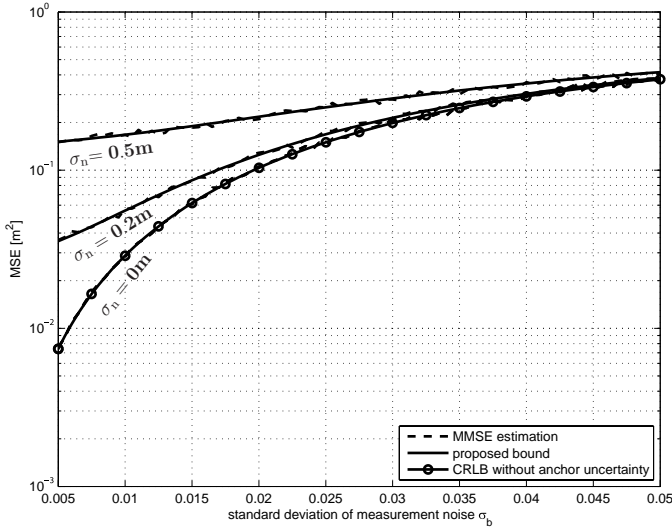


Figure 3. Evaluation of the bound for angle-based localization for an uncertainty on the neighbors' positions varying between $\sigma_n = \{0m, 0.2m, 0.5m\}$.

by (29). In Fig. 2, the bound is shown for range-based localization. In Fig. 3 for angle-based localization. In both Figures it is apparent that the MMSE estimate closely follows the bound (the dashed line representing the estimation error almost coincides with the bound). From this we can conclude that the bound is correct. For $\sigma_n = 0$, the neighbors act as anchors and the bound coincides with the well-known non-cooperative CRLB [10]. It can be seen that an increasing uncertainty of the neighbors' positions increases the bound. Furthermore we observe that as the measurement noise increases the bounds converge irrespective of amount of anchor uncertainty. We can conclude that when the ratio of neighbor uncertainty to measurement noise, i.e., σ_n/σ_r or σ_n/σ_b , goes to zero, the effect of the uncertainty can be neglected. In other words, anchor uncertainty can be considered as a relative quantity and should be expressed with respect to the accuracy of the measurements.

V. SUMMARY AND CONCLUSIONS

In this paper we derive a fundamental bound on the positioning accuracy for hybrid localization with anchor uncertainty.

For this we employ the Bayesian Cramér-Rao lower bound. By exploiting the specific block structure in the FIM, we are able to derive a simple and compact expression for the bound. Simulation results show how the proposed bound can correctly predict the performance of positioning for both distance based and angle based positioning.

ACKNOWLEDGMENTS

The first author gratefully acknowledges the financial support from the Belgian National Fund for Scientific Research (FWO Flanders). This research has been (partly) funded by the Interuniversity Attraction Poles Programme initiated by the Belgian Science Policy Office.

REFERENCES

- [1] M. Kihara and T. Okada, "A satellite selection method and accuracy for the global positioning system," *Navigation*, vol. 31, no. 1, pp. 8–20, 1984.
- [2] M. Zhang and J. Zhang, "A fast satellite selection algorithm: beyond four satellites," *IEEE Journal of Selected Topics in Signal Processing*, vol. 3, no. 5, pp. 740–747, 2009.
- [3] S. Van de Velde, G. Abreu, and H. Steendam, "Frame theory and optimal anchor geometries for wireless localization," in *proc. VTC spring, Seoul*, pp. 1–6, May 2014.
- [4] S. Zhao, B. M. Chen, and T. H. Lee, "Optimal sensor placement for target localisation and tracking in 2d and 3d," *International Journal of Control*, vol. 86, no. 10, pp. 1687–1704, 2013.
- [5] S. M. Kay, *Fundamentals of Statistical signal processing, Volume 2: Detection theory*. Prentice Hall PTR, 1998.
- [6] N. Patwari, A. H. III, M. Perkins, N. S. Correal, and R. J. O'Dea, "Relative location estimation in wireless sensor networks," *IEEE Transactions on Signal Processing*, vol. 51, pp. 2137 – 2148, aug. 2003.
- [7] Y. Shen and M. Win, "Fundamental limits of wideband localization - part I: A general framework," *Information Theory, IEEE Transactions on*, vol. 56, pp. 4956–4980, Oct 2010.
- [8] K. W.-K. Lui, W.-K. Ma, H.-C. So, and F. K. Chan, "Semi-definite programming algorithms for sensor network node localization with uncertainties in anchor positions and/or propagation speed," *Signal Processing, IEEE Transactions on*, vol. 57, no. 2, pp. 752–763, 2009.
- [9] H. Messer, "The hybrid Cramer-Rao lower bound - from practice to theory," in *Sensor Array and Multichannel Processing, 2006. Fourth IEEE Workshop on*, pp. 304–307, 2006.
- [10] N. Patwari, J. N. Ash, S. Kyperountas, A. O. Hero, R. L. Moses, and N. S. Correal, "Locating the nodes: cooperative localization in wireless sensor networks," *Signal Processing Magazine, IEEE*, vol. 22, no. 4, pp. 54–69, 2005.